Two-Dimensional Kagome Lattices Made of Hetero Triangulenes Are Dirac Semimetals or Single-Band Semiconductors

Jing, Y.; Heine, T.;

Originally published:

November 2019

Journal of the American Chemical Society 141(2019)2, 743-747

DOI: https://doi.org/10.1021/jacs.8b09900

Two-dimensional Kagome Lattices Made of Hetero Triangulenes are Dirac Semimetals or Single-Band Semiconductors

Yu Jing[†,‡] and Thomas Heine*[†,‡,§]

[†]Wilhelm-Ostwald-Institut für Physikalische und Theoretische Chemie, Linnéstr. 2, 04103 Leipzig, Germany.

[‡] TU Dresden, Fakultät Chemie und Lebensmittelchemie, Bergstraße 66c, 01062 Dresden, Germany.

[§]Helmholtz-Zentrum Dresden-Rossendorf, Forschungsstelle Leipzig, Permoserstraße 15, 04318 Leipzig, Germany

Supporting Information Placeholder

ABSTRACT: Here we discuss, based on first-principles calculations, two-dimensional (2D) kagome lattices composed of polymerized hetero-triangulene units, planar molecules with D_{3h} point group containing a B, C or N center atom and CH_2, O or CO bridges. We explore the design principles for a functional lattice made of 2D polymers, which involves control of π-conjugation and electronic structure of the knots. The former is achieved by the chemical potential of the bridge groups, while the latter is controlled by the heteroatom. The resulting 2D kagome polymers have a characteristic electronic structure with a Dirac band sandwiched by two flat bands and are either Dirac semimetals (C center), or single-band semiconductors - materials with either exclusively electrons (B center) or holes (N center) as charge carriers of very high mobility, reaching values of up to ~8×10^3 $cm^2V^{-1}s^{-1}$, which is comparable to crystalline silicon.

The properties of a crystalline material are governed by both its lattice geometry and chemical composition. A typical example highlighting the importance of the lattice is the two-dimensional (2D) honeycomb structure of graphene,[1] where the characteristic Dirac cones emerge due to the two hexagonal sub-lattices. Already in 1619 Johannes Kepler reported that only 13 nets with identical knots are possible in two dimensions (as 2 of them are enantiomeric we talk about 11 Kepler nets).[2] Various derivatives of these Kepler nets are possible.[3] However, even fewer than the 11 Kepler nets occur in single-layers exfoliated from natural layered crystals, or on surfaces. As the importance of topology is evident, e.g. from the graphene example, it is intriguing to explore the properties of the remaining Kepler nets and of their derivatives.

It is relatively straight-forward to computationally characterize these artificial lattices,[4] and many interesting properties have been predicted.[5] Enormous efforts were devoted to realize such lattices experimentally,[6] most prominently in photonic lattices.[7] For example, recent experiments confirm the intriguing predicted properties of the Lieb lattice in a challenging ultracold environment,[8] which is a show stopper for real-world applications.

Molecular framework materials, such as metal-organic frameworks (MOFs) and covalent-organic frameworks (COFs), offer new possibilities to form exotic nets,[9] because molecules, acting as knots, can be designed in such way that their bridging sites reflect the required topology of the net. 2D polymers offer the opportunity to create exotic lattices which are stable at ambient conditions, including square,[10] rectangular,[11] honeycomb,[9b,12] and kagome (**kgm**)[13]. 2D polymers have been fabricated by using surface or interface polymerization,[14] and mechanical exfoliation of the layered bulk sometimes is possible.[15] However, in order to realize the desired topological properties of the exotic nets present in the 2D polymers, the molecules marking the knots need to interact electronically with each other. In most cases, the bonds created by the coupling reaction electronically separate the π systems of the monomer units and thus block ballistic charge transport. Full sp^2 conjugation can be achieved if a C=C bond connects the extended monomers to form 2D polymers.[16] Also for the recently reported 2D polymers realized by surface calcination or solution synthesis of hetero-triangulenes (HTs),[17] which form the exotic **kgm** 2D net, intermolecular π conjugation can be expected due to their reported band dispersion.

HTs are nearly planar molecules that have been studied intensively.[18] Our selection for this work is displayed in **Figure 1a-f**. We note that Dirac cones can be anticipated (we confirm them here) in the reported band structures,[17b, 19] even though the HT center atoms, which mark the knots of a honeycomb sublattice, are separated by distances of more than 1 nm.

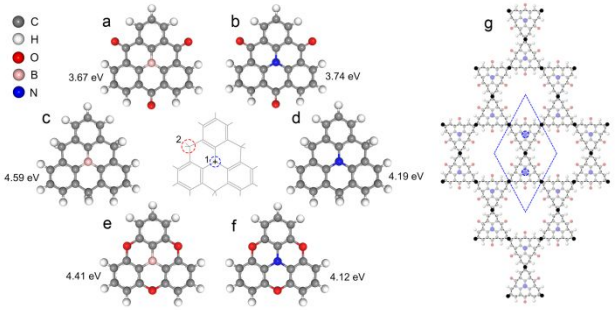

Figure 1. Schematic representation of cationic triangulene (centre) and its HTs derivatives by replacing the centered C^+ (1) with B or N, and the -CH_2 bridge (2) with C=O, or O, respectively, which are (a) carbonyl-bridged triphenylborane (CTPB), (b) carbonyl-bridged triphenylamine (CTPA),[18a] (c) methylene-bridged triphenylborane (MTPB), (d) methylene-bridged triphenylamine (MTPA),[17b] (e) oxygen-bridged triphenylborane (OTPB),[18d] and (f) oxygen-bridged triphenylamine (OTPA).[18e] (g) scheme of the **kgm** lattice that combines a regular hexagonal tiling (blue lattice for the unit cell) and a regular triangular tiling (black lattice).

By using density functional theory (DFT, VASP code,[20a] PAW approach,[20b] cutoff energy of 450 eV, PBE functional,[20c] electronic structure refined by HSE06[20d], details see SI) based

first-principles calculations, we show that 2D HT-based **kgm** lattices exhibit unprecedented electronic features that are accessible by chemical modification of the building units. The HTs act as "superatoms" with local D_{3h} symmetry, in analogy to sp^2 hybridized C atoms. If the center atom is chosen to be carbon (HT(C)), the monomers also electronically act like sp^2 hybridized carbon atoms. Arranging six of them in a "super benzene" structure, we obtain D_{3h} $(HT)_6$ (**Figure S1a**). The frontier π orbitals that resemble the characteristic electronic structure of benzene are prototypic for aromatic molecules. Arranged in an extended 2D **kgm** lattice (**Figure S1b**), the electronic structure includes the expected half-filled Dirac cones at the K points of the Brillouin zone which emerge from the honeycomb sublattice (**Figure S1c**). If the heteroatoms are changed to B or N, the resulting **kgm** lattices show a peculiar combination of two apparently mutually exclusive characteristics: one of the bands next to the Fermi level is flat and does not contribute to charge transport, the other one is strongly dispersed, with highly mobile charge carriers (reaching mobility of 8×10^3 $cm^2V^{-1}s^{-1}$ in the case of **kgm** CTPB-polymer), and thus determines the electric conductivity. The **kgm** HT-polymers become either n-type (only electrons as mobile charge carriers) or p-type (only holes as mobile charge carriers) single band (intrinsic) semiconductors, by either completely emptying (B) or filling (N) the strongly dispersed Dirac bands (**Figure S1c**).

Highly reactive triangulene is a π radical with two unpaired electrons.[21] Stable cationic closed-shell derivatives are obtained by substitution of outer CH groups with CO, O, or CH_2 bridges (**Figure 1**). Such molecular ions have been widely used as dyes.[22] As neutral, single radical species, their D_{3h} symmetry allows the arrangement in a **kgm** lattice as shown in **Figure 1g**, thus forming a **kgm** 2D polymer with a honeycomb sublattice that carries the HT center atoms. The frontier orbital of the HT(C)s has π character with one unpaired electron and resembles the electronic features of sp^2 carbons in aromatic molecules, illustrated for the benzene-analogue of CTP in **Figure S1a**. The HT(C) atoms forming the honeycomb sublattice yield a band resembling the graphene electronic structure with Dirac cones at the K points of the Brillouin zone (**Figure 2 b, e, h**), even though their distance is ~ 1 nm, seven times larger than in graphene. In free-standing form, for steric reasons, the monomers are slightly twisted with respect to one another, which results in the opening of a small band gap of 29~58 meV (**Figure S2**).

On the other hand, the substituted HTs resemble the electronic analogues of 2D nitrogen (N-substituted) and 2D boron (B-substituted), both in the honeycomb sublattice. The six substituted HT(N/B) structures are shown in **Figure 1a-f**, all of these molecules being nearly planar and with HOMO-LUMO gaps in the range of 3.7-4.6 eV. The resulting **kgm** HT(N/B)-polymers are stable (two have been reported experimentally),[17a,b] and for all others the reaction energy is very similar, ranging from 1.36...1.86 eV/unit (see **Equation S1**, **Table S1** and **Figure S3**). They all have similar lattice vectors (17.07…17.62 Å) and pore sizes (11.75…13.10 Å) (**Table S1**). In free-standing form, the **kgm** HT(N/B)-polymers are slightly twisted. In the remainder, however, we assume them to adopt flat geometries in agreement with a suspended structure as expected in experiment (see refs. 17a,b). However, even if they are slightly twisted, their electronic characteristics are maintained and the twisting has negligible impact on the results presented and discussed here (for details, see **Figure S4** and **Table S1** and **S2**).

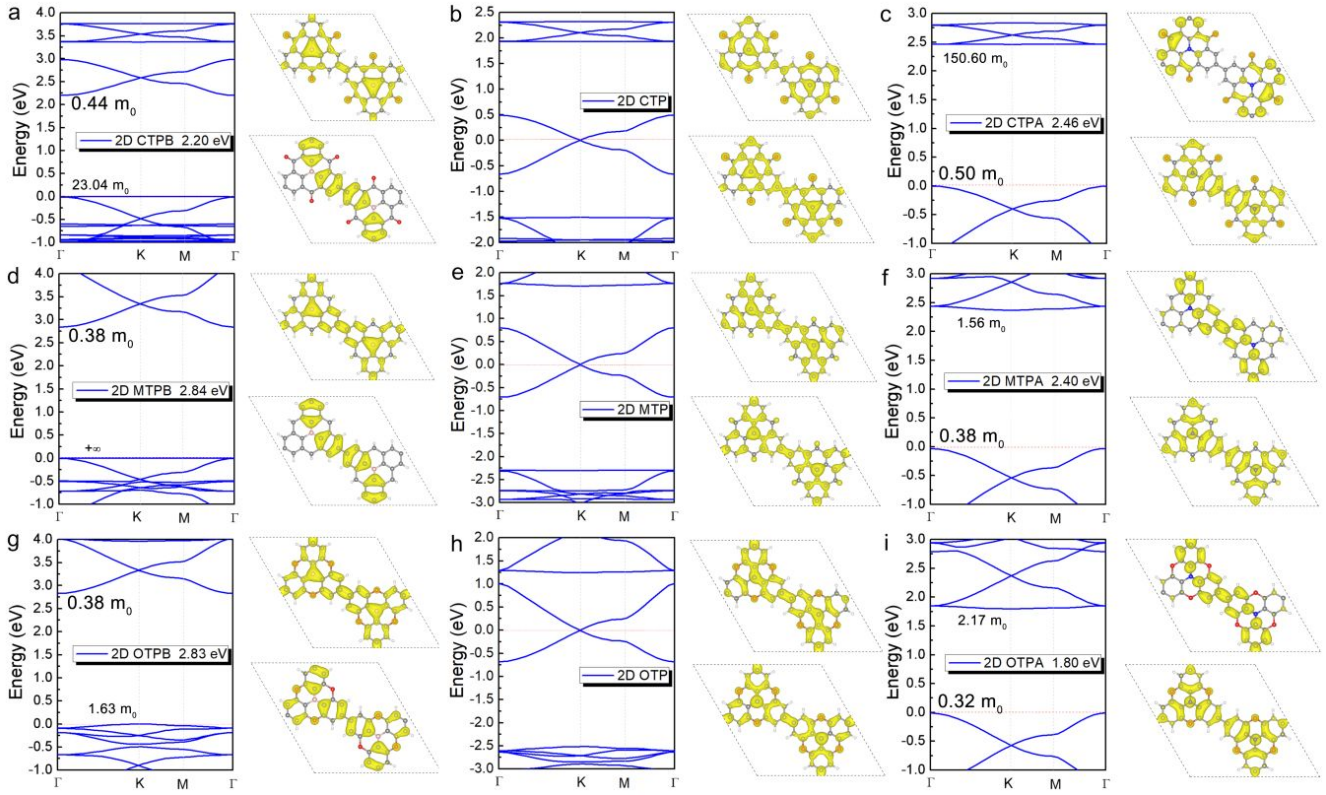

Figure 2. (a-i) band structures, at the HSE06 level and corresponding charge density distribution for CBM (above) and VBM (below), respectively, of **kgm** HT(B/C/N)-polymers (their monomers are introduced in **Figure 1a-f**). 2D MTP and OTP complete the **kgm** HT(C)-polymers built from MTP radical and OTP radical. The Fermi level is set at the VBM for the semiconductors, effective masses of the frontier bands are indicated, and the isosurface for all orbitals is set to be 0.0013 $eÅ^{-3}$. All structures are spin unpolarized.

Table 1. Calculated effective masses m* for electrons and holes (italic values indicate low-mobility carriers) at the PBE level. For the mobile charge carriers, deformation potential (DP) constant E_1, in-plane stiffness C_{2D} and carrier mobility μ for **kgm** HT(N/B)-polymers along the zigzag direction. Armchair values differ only slightly (see **Table S4**).

kgm HT-polymers	CTPB	CTPA	MTPB	MTPA	OTPB	OTPA
m_e^*/m_0	0.44	*150.60*	0.34	*1.56*	0.35	*2.17*
m_h^*/m_0	*23.04*	0.47	∞	0.30	*1.63*	0.27
E_1 /eV	0.72	2.21	2.09	3.87	2.97	4.78
C_{2D} /Nm^{-1}	59.32	63.25	59.79	62.73	65.05	63.72
μ /× 10^3 cm^{2}V^{-1}s^{-1}	8.39	0.83	1.68	0.66	0.85	0.54

According to their band structures, the triangulene-based **kgm** polymers can be categorized in two classes (**Figure 2**): **kgm** HT(C)-polymers are Dirac semimetals, and the **kgm** HT(N/B)-polymers are intrinsic single-band semiconductors with electrons (HT(B)-polymers) and holes (HT(N)-polymers) as mobile charge carriers. Note that for **kgm** HT(C)-polymers a tiny band gap of ~0.05 meV is observed when spin-orbit coupling is included in the Hamiltonian, a value similar as found for graphene. This indicates a topological phase for 2D HT(C) polymers. The band gaps range from 1.8-2.8 eV, with the band edges being enclosed within the HOMO-LUMO region of their corresponding HT(N/B) monomers (**Figure S5**). In all cases, the flat bands have their extrema (if they can be specified) at the K point, while those of the strongly dispersed band are located at the Γ point. Even though the effective masses of the mobile charge carriers are similar, ranging from 0.32-0.5 m_0 (**Figure 2**, **Table S3**), the calculated charge carrier mobilities (see **Equation S2**, **Table 1**, **Figure S6**) differ strongly between the **kgm** HT(N)-polymers (0.5-0.9×10^3 cm^{2}V^{-1}s^{-1}) and their generally more mobile HT(B)-polymer counterparts (0.8-8.4 ×10^3 cm^{2}V^{-1}s^{-1}). For the flat bands, the lowest effective masses are 1.6 m_0, while for some structures the effective masses exceed 100 m_0.

The honeycomb sublattice makes the HTs behave like "sp^2–superatoms" B, C and N, where the sp^2–like configuration is enforced by the D_{3h} symmetry and planarity of the HTs, with a π-orbital (resembling the $2p_z$) that is either empty (B), half-filled (C) or filled (N). Orbitals of the flat bands (**Figure S7**) show no contribution of the HT center atoms (independent of C, N or B), but are delocalized on the remainder of the 2D lattice. Bridge functionalization controls the orbital shapes of the HT(N/B) molecules and thus the conjugation in the **kgm** HT(N/B)-polymers, in particular the curvature of the flat bands. In the case of very flat bands (VB of **kgm** CTPB-polymer and MTPB-polymer, CB of **kgm** CTPA-polymer) the π electron density is significant at the bridge groups, but reduces at the bonds connecting the monomers (**Figure 2**). Appreciable conjugation is observed for the more dispersed flat bands (VB of **kgm** OTPB-polymer, CB of **kgm** MTPA-polymer and OTPA-polymer). Partial density-of-states analysis (**Figure S8**) indicates that the C=O bridge has significant contribution at the VBM of **kgm** CTPB-polymer and CBM of CTPA-polymer, contrary to CH_2 and O bridges. The conjugated band with the low-effective-mass charge carriers is less affected, but this picture changes for charge carrier mobilities, where both center atom and bridge group strongly affect the electron-phonon coupling via the deformation potential: the holes in **kgm** HT(N)-polymers are more prone to acoustic phonon scattering than the electrons of **kgm** HT(B)-polymers that possess the same bridge skeleton, while the C=O, CH_2 and O bridges reduce the carrier mobilities in that order, but with smaller impact. Note that due to neglect of coupling between optical phonons and electrons our predicted charge carrier mobilities are likely to be slightly overestimated.

To summarize, we have shown that hetero-triangulene derivatives form kagome lattices which show a peculiar electronic structure of a Dirac band sandwiched by two flat bands. The center atoms of the HTs mark a honeycomb sublattice, and act like sp^2 "superatoms" B, C or N. Although they are ~1 nm apart from each other, they still interact considerably, which results in the highly dispersed Dirac band which contains the mobile charge carriers of the presented 2D polymers. The six **kgm** HT(B/N)-polymers are intrinsic semiconductors with band gaps in the range of 1.8-2.8 eV. The center atom (B or N) determines the type of mobile charge carrier, while the bridge functional group influences the flat band curvature via π conjugation, and the band gap. While one frontier band shows very high charge carrier mobility of up to 8 ×10^3 cm^{2}V^{-1}s^{-1}, the other bands do not contribute to charge transport. Those flat bands contribute high peaks in the electronic density-of-states and may offer interesting phenomena, e.g. Lifshitz transitions,[23] if located at the Fermi level. Our observations suggest that the flat bands are inherent features of the **kgm** lattice, as their crystal orbitals are formed by all atoms except for the center ones, and as their dispersion is strongly influenced by the bridge groups which mark the edges of the triangles that characterize the **kgm** lattice structure.

ASSOCIATED CONTENT

Supporting Information

The Supporting Information is available free of charge via the Internet at http://pubs.acs.org.
Details of the DFT calculations, frontier orbitals of HTs oligomers, stability of **kgm** HT(N/B)-polymers, band structure of twisted **kgm** HT-polymers and details for the calculations of the carrier mobilities according to the DP theory, orbitals of the flat bands and density of states of **kgm** HT(N/B)-polymers are given in the Supporting information.

AUTHOR INFORMATION

Corresponding Author

*thomas.heine@tu-dresden.de

ORCID

Yu Jing: 0000-0002-1537-9522
Thomas Heine: 0000-0003-2379-6251

Notes

The authors declare no competing financial interests.

ACKNOWLEDGMENT

The authors are grateful to the financial support by FlagERA (DFG HE 3543/27-1) and by the H2020 Marie Skłodowska–Curie Actions (H2020-MSCA-IF-2016, No.751848). We thank ZIH Dresden for computer time.

REFERENCES

(1) Novoselov, K. S.; Geim1, A. K.; Morozov, S. V.; Jiang, D.; Katsnelson, M. I.; Grigorieva, I. V.; Dubonos, S. V.; Firsov, A. A. Two-dimensional gas of massless Dirac fermions in grapheme. *Nature* **2005**, *438*, 197-200.
(2) (a) Kepler, J. Weltharmonik II. Buch der Weltharmonik. München – Berlin: R. Oldenbourg Verlag, **1939**, P. 63; Original: Harmonice Mundi, 1619.(b) Coxeter, H. S. M. Regular polytopes, Dover Publications: Third Edition, New York, **1973**, P. 14, 69, 149.

(3) Smirnova, N. L. On Kepler-Shubnikov nets. *Crystallogr. Rep*. **2009**, *54*, 743.
(4) (a) Delplace, P.; Ullmo, D.; Montambaux, G. Zak phase and the existence of edge states in graphene. *Phys. Rev. B* **2011**, *84*, 195452. (b) Liu, Z.; Wang, Z. F.; Mei, J. W.; Wu, Y. S.; Liu, F. Flat chern band in a two-dimensional organometallic framework. *Phys. Rev. Lett.* **2013**, *110*, 106804. (c) Liu, F.; Wakabayashi, K. Novel Topological Phase with a Zero Berry Curvature. *Phys. Rev. Lett*. **2017**, *118*, 076803. (d) Gouveia, J. D.; Maceira, I. A.; Dias, R. G. Evolution of localized states in Lieb lattices under time-dependent magnetic fields. *Phys. Rev. B* **2016**, *94*, 195132.
(5) (a) Terrones, H.; Terrones, M.; Hernandez, E.; Grobert, N.; Charlier, J. C.; Ajayan, P. M. New metallic allotropes of planar and tubular carbon. *Phys. Rev. Lett*. **2000**, *84*, 1716. (b) Weeks, C.; Franz, M. Topological insulators on the Lieb and perovskite lattices. *Phys. Rev. B* **2010**, *82*, 085310. (c) Dias, R. G.; Gouveia, J. D. Origami rules for the construction of localized eigenstates of the Hubbard model in decorated lattices. *Sci. Rep*. **2015**, *5*, 16852. (d) Goldman, N.; Urban, D. F.; Bercioux, D. Topological phases for fermionic cold atoms on the Lieb lattice. *Phys. Rev. A* **2011**, *83*, 063601. (e) Van Miert, G; Smith, C. M. Dirac cones beyond the honeycomb lattice: A symmetry-based approach. *Phys. Rev. B* **2016**, *93*, 035401.
(6) (a) Sarkar, S.; Langer, S; Schachenmayer, J.; Daley, A. J. Light scattering and dissipative dynamics of many fermionic atoms in an optical lattice. *Phys. Rev. A* **2014**, *90*, 023618. (b) Schachenmayer, J.; Weld, D. M.; Miyake, H.; Siviloglou, G. A.; Ketterle, W.; Daley, A. J. Adiabatic cooling of bosons in lattices to magnetically ordered quantum states. *Phys. Rev. A***2015**, *92*, 041602. (c) Kantian, A.; Langer, S.; Daley, A. J. Dynamical disentangling and cooling of atoms in bilayer optical lattices. *Phys. Rev. Lett*. **2018**, *120*, 060401.
(7) (a) Vicencio, R.; Cantillano, C.; Morales-Inostroza, L.; Real, B.; Mejía-Cortés, C.; Weimann, S.; Szameit, A.; Molina, M. I. Observation of localized states in Lieb photonic lattices. *Phys. Rev. Lett*. **2015**, *114*, 245503. (b) Mukherjee, S.; Spracklen, A.; Choudhury, D.; Goldman, N.; Öhberg, P.; Andersson, E.; Thomson, R. R. Observation of a localized flat-band state in a photonic Lieb lattice. *Phys. Rev. Lett*. **2015**, *114*, 245504 .
(8) (a) Slot, M. R.; Gardenier, T. S.; Jacobse, P. H.; van Miert, G. C.; Kempkes, S. N.; Zevenhuizen, S. J.; Smith, C. M.; Vanmaekelbergh, D.; Swart, I. Experimental realization and characterization of an electronic Lieb lattice. *Nat. Phy*. **2017**, *13*, 672-676. (b) Drost, R.; Ojanen, T.; Harju, A.; Liljeroth, P. Topological states in engineered atomic lattices. *Nat. Phys*. **2017**, *13*, 668-671. (c) Bercioux, D.; Otte S. Solid-state platforms. *Nat. Phys*. **2017**, *13*, 628-629.
(9) (a) Li, H.; Eddaoudi, M.; O'Keeffe, M.; Yaghi, O. M. Design and synthesis of an exceptionally stable and highly porous metal-organic framework. *Nature* **1999**, *402*, 276. (b) Côté, A. P.; Benin, A. I.; Ockwig, N.W.; Keeffe, M.; Matzger, A. J.; Yaghi, O. M. Porous, crystalline, covalent organic frameworks. *Science* **2005**, *18*, 1166-1170.
(10) Kandambeth, S.; Shinde, D. B.; Panda, M. K.; Lukose, B.; Heine, T.; Banerjee, R. Enhancement of chemical stability and crystallinity in porphyrin-containing covalent organic frameworks by intramolecular hydrogen bonds. *Angew. Chem*. **2013**, *125*, 13290-13294.
(11) Huang, N.; Zhai, L.; Coupry, D. E.; Addicoat, M. A.; Okushita, K.; Nishimura, K.; Heine, T.; Jiang, D. Multiple-component covalent organic frameworks. *Nat. Comm*. **2016**, *7*, 12325.
(12) Kandambeth, S.; Mallick, A.; Lukose, B.; Mane, M. V.; Heine, T.; Banerjee, R. Construction of crystalline 2D covalent organic frameworks with remarkable chemical (acid/base) stability via a combined reversible and irreversible route. *J. Am. Chem. Soc*. **2012**, *134*, 19524-19527.
(13) (a) Huang, N.; Wang, P.; Jiang, D. Covalent organic frameworks: a materials platform for structural and functional designs. *Nat. Rev. Mater*. **2016**, *1*, 16068. (b) Feng, X.; Ding, X.; Jiang, D. Covalent organic frameworks. *Chem. Soc. Rev*. **2012**, *41*, 6010-6022. (c) Waller, P. J.; Gándara, F; Yaghi, O. M. Chemistry of covalent organic frameworks. *Acc. Chem. Res*. **2015**, *48*, 3053-3063. (d) Tang, E.; Mei, J.-W.; Wen, X.-G. High-temperature fractional quantum hall states. *Phys. Rev. Lett*. **2011**, *106*, 236802. (e) Kambe, T.; Sakamoto, R.; Hoshiko, K.; Takada, K.; Miyachi, M.; Ryu, J.-H.; Sasaki, S.; Kim, J.; Nakazato, K.; Takata, M.; Nishihara, H. π-Conjugated Nickel Bis(dithiolene) Complex Nanosheet. *J. Am. Chem. Soc*. **2013**, *135*, 2462−2465. (f) Wang, Z. F.; Su, N.; Liu, F. Prediction of a two-dimensional organic topological insulator. *Nano Lett*. **2013**, *13*, 2842−2845.(g) Mielke, A. Exact ground states for the Hubbard model on the Kagome lattice. *J. Phys. A: Math. Gen*. **1992**, *25*, 4335. (h) Shiraishi, K.; Tamura, H.; Takayanagi, H. Design of a semiconductor ferromagnet in a quantum-dot artificial crystal. *Appl. Phys. Lett*. **2001**, *78*, 3702-3704.
(14) (a) Xu, L.; Zhou, X.; Tian, W. Q.; Gao, T.; Zhang, Y. F.; Lei, S.; Liu, Z. F. Surface-confined single-layer covalent organic framework on single-layer graphene grown on copper foil. *Angew. Chem. Int. Ed*. **2014**, *53*, 9564-9568. (b) Liu, X. H.; Guan, C. Z.; Ding, S. Y.; Wang, W.; Yan, H.-J.; Wang, D.; Wan, L. J. On-surface synthesis of single-layered two-dimensional covalent organic frameworks via solid–vapor interface reactions. *J. Am. Chem. Soc*. **2013**, *135*, 10470-10474. (c) Dai, W.; Shao, F.; Szczerbiński, J.; McCaffrey, R.; Zenobi, R.; Jin, Y.; Schlüter, A. D.; Zhang, W. Synthesis of a two-dimensional covalent organic monolayer through dynamic imine chemistry at the air/water interface. *Angew. Chem. Int. Ed*. **2016**, *55*, 213-217. (d) Müller, V.; Shao, F.; Baljozovic, M.; Moradi, M.; Zhang, Y.; Jung, T.; Thompson, W. B.; King, B. T.; Zenobi, R.; Schlüter, A. D. Structural characterization of a covalent monolayer sheet obtained by two-dimensional polymerization at an air/water Interface. *Angew. Chem. Int. Ed*. **2017**, *56*, 15262-15266. (e) Wang, W.; Schlüter, A. D. Synthetic 2D polymers: Looking into the future. *Macromol. Rapid Commun*. **2018**, 1800719.
(15) (a) Biswal, B. P.; Chandra, S.; Kandambeth, S.; Lukose, B.; Heine, T.; Banerjee, R. Mechanochemical synthesis of chemically stable isoreticular covalent organic frameworks. *J. Am. Chem. Soc*. **2013**, *135*, 5328-5331. (b) Chandra, S.; Kandambeth, S.; Biswal, B. P.; Lukose, B.; Kunjir, S. M.; Chaudhary, M.; Babarao, R.; Heine, T.; Banerjee, R. Chemically stable multilayered covalent organic nanosheets from covalent organic frameworks via mechanical delamination. *J. Am. Chem. Soc*. **2013**, *135*, 17853-17861.
(16) (a) Jin, E.; Asada, M.; Xu, Q.; Dalapati, S.; Addicoat, M. A.; Brady, M. A.; Xu, H.; Nakamura, T.; Heine, T.; Chen, Q.; Jiang, D. Two-dimensional sp^2 carbon–conjugated covalent organic frameworks. *Science* **2017**, *357*, 673-676. (b) Zhuang, X.; Zhao, W.; Zhang, F.; Cao, Y.; Liu, F.; Bi, S.; Feng, X. A two-dimensional conjugated polymer framework with fully sp2-bonded carbon skeleton. *Polym. Chem*. **2016**, *7*, 4176-4181.
(17) (a) Bieri, M.; Blankenburg, S.; Kivala, M.; Pignedoli, C. A.; Ruffieux, P.; Müllen, K.; Fasel, R. Surface-supported 2D heterotriangulene polymers. *Chem. Commun*. **2011**, *47*, 10239-10241. (b) Steiner, C.; Gebhardt, J.; Ammon, M.; Yang, Z.; Heidenreich, A.; Hammer, N.; Görling, A.; Kivala, M.; Maier, S. Hierarchical on-surface synthesis and electronic structure of carbonyl-functionalized one- and two-dimensional covalent nanoarchitectures. *Nature Comm*. **2017**, *8*, 14765. (c) Schlütter, F.; Rossel, F.; Kivala, M.; Enkelmann, V.; Gisselbrecht, J.-P.; Ruffieux, P.; Fasel, R.; Müllen, K. π-Conjugated Heterotriangulene Macrocycles by Solution and Surface-supported Synthesis toward Honeycomb Networks. *J. Am. Chem. Soc*. **2013**, *135*, 4550-4557.
(18) (a) Field, J. E.; Venkataraman, D. Heterotriangulenes-structure and properties. *Chem. Mater*. **2002**, *14*, 962-964.(b) Zhou, Z.; Wakamiya, A.; Kushida, T.; Yamaguchi, S. Planarized triarylboranes: stabilization by structural constraint and their plane-to-bowl conversion. *J. Am. Chem. Soc*. **2012**, *134*, 4529-4532. (c) Hellwinkel, D.; Melan, M. Heteropolycyclen vom triangulen-typ, II. zur stereochemie verbrückter triarylamine. *Chem. Ber*. **1974**, *107*, 616. (d) Kitamoto, Y.; Suzuki, T.; Miyata, Y.; Kita, H.; Funaki, K.; Shuichi, O. The first synthesis and X-ray crystallographic analysis of an oxygen-bridged planarized triphenylborane. *Chem. Commun*. **2016**, *52*, 7098-7101. (e) Kuratsu, M.; Kozaki, M.; Okada, K. 2,2′:6′,2″:6″,6-Trioxytriphenylamine: synthesis and properties of the radical cation and neutral species. *Angew. Chem. Int. Ed.* **2005**, *44*, 4056-4058.
(19) Gutzler, R. Band-structure engineering in conjugated 2D polymers. *Phys. Chem. Chem. Phys*. **2016**, *18*, 29092-29100.
(20) (a) Kresse, G.; Hafner, J. Ab initio molecular dynamics for liquid metals. *Phys. Rev. B: Condens. Matter Mater. Phys*. **1993**, *47*, 558-561. (b) Blöchl, P. E. Projector augmented-wave method. *Phys. Rev. B: Condens. Matter Mater. Phys.* **1994**, *50*, 17953-17979. (c) Perdew, J. P.; Burke, K.; Ernzerhof, M. Generalized gradient approximation made simple. *Phys. Rev. Lett*. **1996**, *77*, 3865-3868. (d) Heyd, J.; Peralta, J. E.; Scuseria, G. E.; Martin, R. L. Energy band gaps and lattice parameters evaluated with the Heyd-Scuseria-Ernzerhof screened hybrid functional. *J. Chem. Phys*. **2005**, *123*, 174101.
(21) Pavliček, N.; Mistry, A.; Majzik, Z.; Moll, N.; Meyer, G.; Fox, D. J.; Gross, L. Synthesis and characterization of triangulene. *Nature Nanotech*. **2017**, *12*, 308-311.
(22) Bosson, J.; Gouin, J.; Lacour, J. Cationic triangulenes and helicenes: synthesis, chemical stability, optical properties and extended applications of these unusual dyes. *Chem. Soc. Rev*. **2014**, *43*, 2824-2840.
(23) Lifshitz, I. M. Anomalies of electron characteristics of a metal in the high pressure region. J. *Exptl. Theoret. Phys.(U.S.S.R.)***1960**, *38*, 1569-1576.

Table of Contents artwork